

A new wavefront sensor for Keck: Pyramid wavefront sensing in the near infrared

Charlotte Z. Bond^a, Sylvain Cetre^b, Sam Ragland^b, Scott Lilley^b, Peter Wizinowich^b, Dimitri Mawet^c, Mark Chun^a, Jacques-Robert Delorme^c, Nemanja Jovanovic^c, Edward Wetherell^b, Shane Jacobson^a, Charles Lockhart^a, Eric Warmbier^a, James K. Wallace^f, Donald N. Hall^a, Sean Goebel^a, and Olivier Guyon^d

^aInstitute for Astronomy, University of Hawaii, 640 N. Aohoku Place, Hilo, HI 96720, USA.

^bW. M. Keck Observatory, 65 - 1120 Mamalahoa Hwy., Kamuela, HI 96743, USA.

^cDepartment of Astronomy, California Institute of Technology, Pasadena, CA 91106, USA

^dSubaru Telescope NAOJ, 650 N. Aohoku Place, Hilo, HI 96720, USA

^eINAF Osservatorio Astronomico di Arcetri, 50125 Firenze, Italy

^fJet Propulsion Laboratory, California Institute of Technology, Pasadena, CA 91109, USA

ABSTRACT

A near infrared pyramid wavefront sensor (WFS) has been successfully installed on the Keck II telescope as part of the Keck Planet Imager and Characterizer (KPIC). The combination of the highly sensitive pyramid WFS and low noise infrared detector technology (specifically the SAPHIRA APD array) is opening up new opportunities for high resolution, high contrast imaging of faint red objects. Such capability will allow the detailed study of phenomena such as exoplanets around M-dwarf stars and planet formation in obscured star forming regions. This system is the first of its kind (an infrared pyramid WFS implemented on a 10 m class telescope), providing insight for future adaptive optics (AO) systems such as those planned for the Extremely Large Telescopes.

In this paper we present an overview of this new wavefront sensor, including the results of commissioning and the science verification process. We explore the benefits of operating a pyramid WFS in the infrared and the new capabilities provided by such a system. In addition, we compare the current performance with that of Keck's facility AO systems.

Keywords: wavefront sensing, infrared, adaptive optics

1. INTRODUCTION

Wavefront sensing in the infrared is highly desirable for astrophysics observations using adaptive optics (AO) systems. Many particularly compelling science cases involve cool, red objects which are often too faint to use as the natural guide star (NGS) for visible wavefront sensing but bright enough at infrared wavelengths. Advancements in infrared technology have resulted in low noise ($< 1 e^-$), high speed (> 1 kHz) infrared detectors, which can now enable infrared wavefront sensing.

Developments in AO have led to the emergence of the pyramid wavefront sensor (WFS) as the leading sensor to enable high contrast instruments. Previous implementations of visible pyramid WFSs on large telescopes have demonstrated the high sensitivity and contrasts achievable with such sensors.¹⁻³ In addition, the increased sensitivity of the pyramid WFS, compared to the industry standard Shack-Hartmann sensor, can extend AO performance to fainter guide stars. Combining a pyramid sensor with low-noise infrared detector technology allows for AO correction of objects that are faint at visible wavelengths but relatively bright in the infrared. This is a significant advantage over other AO systems, where the study of red objects requires an off-axis visible NGS or use of laser guide star (LGS) AO, both of which provide sub-optimal correction of the science object.

In this paper we present the new infrared pyramid WFS recently installed on the Keck II telescope. We discuss the benefits and novelty of the first infrared pyramid implemented on a 10 m telescope and present results from on-sky commissioning and initial science verification.

Further author information: (Send correspondence to C. Z. Bond)

E-mail: czbond@hawaii.edu

2. THE KECK PLANET IMAGER AND CHARACTERIZER

The Keck Planet Imager and Characterizer (KPIC)^{4,5} is a new instrument for the Keck Observatory which provides high resolution images of cool, red objects. In particular the instrument aims to observe objects thought to be promising grounds for the study of planet formation: M-dwarf systems and associated exoplanets and young planets in proto-planetary discs. In addition to direct imaging a key goal of KPIC is to take spectra of known - previously imaged - exoplanets, separating the light of the planet from its host star using a fiber injection unit (FIU)⁶ attached to a high resolution spectrograph. Such measurements will provide invaluable information about the composition of planetary atmospheres.

A crucial part of this instrument is the infrared pyramid WFS, which provides the high resolution AO sensing required for both direct imaging and spectroscopy via the FIU. Currently the pyramid WFS is used to control the 21×21 deformable mirror (DM) of the Keck facility AO system. In a second phase of the KPIC project an independent higher order MEMS DM will be used to provide the correction for the FIU.

2.1 Infrared pyramid wavefront sensing

The pyramid WFS uses a prism 4-sided in the focal plane of the telescope and re-imaging optics to produce 4 images of the telescope pupil on the WFS detector.⁷ The distribution of light within the pupil images is then used to reconstruct the wavefront and feedback commands to the DM. Studies of the pyramid WFS have demonstrated it's improved sensitivity over the standard Shack-Hartmann sensor.⁸ However, this high sensitivity comes at the expense of a small range of linear operation. The linear range of the sensor can be adjusted by *modulation*, a circular motion of the focal plane which effectively produces a larger 'spot' at the pyramid tip - increasing the range of the sensor but reducing the sensitivity.

The choice of infrared wavefront sensing is primarily motivated by the science cases of interest. For KPIC these are objects typically faint in the visible, but bright enough in the infrared to be used for infrared wavefront sensing. This allows for optimal correction for these particular science cases and, for such sources, increases the sky coverage of the AO system.^{4,9} In addition to the scientific motivation, there are benefits specific to the pyramid WFS in using the infrared: the sensor is less susceptible to non-linear effects at longer wavelengths. The high sensitivity of the pyramid, as discussed above, is the case for a diffraction limited PSF, or very small deviations from this. Any effect which distorts the closed loop PSF will result in a reduction of sensitivity. In the case of a visible pyramid WFS this effect can be significant, altering the sensitivity of the sensor during on-sky operation and often requiring modal gain adjustments or on-sky calibration to compensate.¹⁰ Going to longer wavelengths - the infrared - produces a better corrected PSF on the tip of the pyramid and significantly reduces these non-linear effects, allowing the system to operate close to its design sensitivity on-sky.

3. THE KECK PYRAMID WFS

3.1 Design

The detailed design of the Keck pyramid WFS was completed in September 2017. The optical and mechanical design is presented in detail in Lilley et al. (2018),¹¹ and the design of the real-time controller (RTC) is described in Cetre et al. (2018).¹² Here we will highlight several crucial aspects of the design.

3.1.1 Wavefront sampling

One critical design choice is the sampling of the wavefront. In the case of a pyramid WFS the sampling of the wavefront is given by the number of pixels across the individual pupil images - see figure 1. This depends on the physical size of the pupils - determined by the incoming f-ratio and focal length of the re-imaging optics - and the physical size of the detector pixels. Careful choice of the optical parameters with respect to the pixel size allows for a chosen wavefront sampling. For the Keck pyramid WFS a minimum sampling of 32 pixels is required to match the 32 DM actuators across the pupil of the phase II KPIC design. However, additional considerations suggest oversampling the pupil is preferred, specifically the positioning of the four pupils on the detector. Our preferred method for wavefront control is a combination of the four pupil images into *slope* maps. In the case where the four pupil images are not separated by an integer number of pixels the fraction of a pixel shift can cause the sensor to become less sensitive to high spatial frequencies in the wavefront. For large shifts (up to

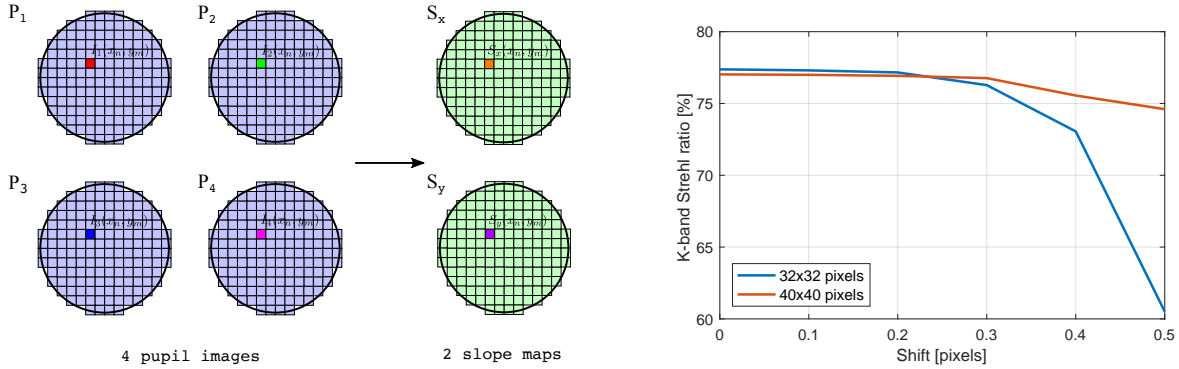


Figure 1. Wavefront sampling with a pyramid WFS. **Left:** Illustration of 4 pyramid pupils imaged onto a detector and the associated slope maps computed by combining the pupil images using a quad cell formula. **Right:** Results from a simulation of the Keck pyramid WFS, showing the performance versus the relative shifts of the pupil images on the detector, for different wavefront sampling.

0.5 pixels) these modes can become unstable and uncontrollable. Achieving a separation of an integer number of pixels requires incredibly high precision on the angle of prisms. However, this effect can be largely mitigated by slightly over-sampling with respect to the number of actuators. The results of simulations of this effect are shown in figure 1 for samplings of 32 and 40 pixels using the higher order DM (32 actuators). In the case of a large fractional shift between the pupils the higher sampling mitigates the impact on performance. From this study the decision was made to over sample the wavefront, with 40 pixels across the Keck pupil.

Further detailed simulations were carried out to inform other design decisions and determine the expected performance of the system. These are summarised in Plantet et al. (2018).¹³

3.1.2 Choice of detector

The choice of infrared detector is crucial in determining the eventual sensitivity of the sensor and the limiting magnitude of the AO system. For KPIC we took advantage of the infrared detector developments at the University of Hawaii’s Institute for Astronomy (IfA), specifically the SAPHIRA infrared avalanche photodiode array. This detector has demonstrated the low noise ($<1 e^-$) required, along with high speeds (>1 kHz) when operating in sub-array mode.^{14,15} The Keck pyramid was designed to do the wavefront sensing in H-band, with an additional thermal blocking filter installed within the SAPHIRA cryostat.

The detector is used in conjunction with a custom Pizzabox controller, specifically developed at the IfA to meet the requirements for a pyramid WFS. This involved developing a read mode which is synchronized with the pyramid modulation.

3.1.3 Optical and mechanical design

The left panel of figure 2 shows an illustration of the optical layout of the Keck pyramid WFS. The main considerations for the optical design were to provide the required optical planes at the correct sizes and to produce the desired sampling of the wavefront (see above). The system required two pupil planes within the optical relay: one for the pyramid modulator and one for the future KPIC DM, both with a pupil size of 12.3 mm (determined by the size of the higher order DM chosen for phase II). A combination of lenses was selected to provide the chosen wavefront sampling of each pupil: 40 pixels across with a separation of 65 pixels. This allows the four pupils to fit within a 128×128 sub-array of the SAPHIRA detector, allowing for frame rates up to 1.5 kHz.

Figure 2 also shows an image of the CAD model of the mechanical design of the pyramid WFS plate, excluding the SAPHIRA camera and associated mechanics. The two sub-systems of KPIC (the pyramid WFS and FIU) each have their own plate, with the majority of the J- and H-band light sent to the WFS. The two plates are then mounted on a common baseplate via kinematic mounts. This allows for individual installation on the AO bench - a crucial requirement due to space constraints - whilst maintaining the internal alignment of the combined system.

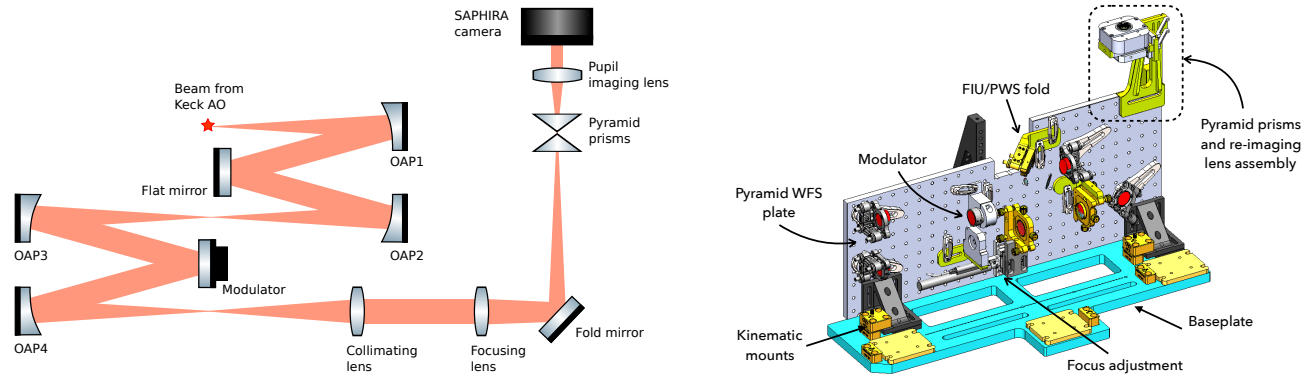


Figure 2. Design of the Keck pyramid WFS. **Left:** Illustration of the optical design of the Keck pyramid WFS. **Right:** CAD model of the pyramid WFS plate. The WFS plate and FIU plate (not shown here) are mounted on a common baseplate.

3.2 Laboratory testing

In March 2018 the two KPIC subsystems - the pyramid WFS and FIU - were integrated at the IfA in Hilo. The final instrument is shown in the left panel of figure 3. The system was thoroughly tested in the lab, including:

1. measuring the response of the dynamic components: the modulator, focus stage and pupil stabilization system;
2. characterizing the SAPHIRA detector and measuring the associated noise;
3. checking the co-alignment of the pyramid WFS and FIU and confirming a wavefront error below 30 nm rms.

Figure 3 shows an example of a measurement taken to characterize the SAPHIRA: the avalanche gain of the detector versus the voltage bias. This is a crucial parameter in determining the effective read noise of the detector. Noise measurements determined an avalanche gain of ~ 55 would provide effective sub-electron read noise in the lab, with a slightly higher gain of ~ 75 required once the camera was installed on the Keck II AO bench. These gains are easily achievable with the SAPHIRA detector, as shown in figure 3.

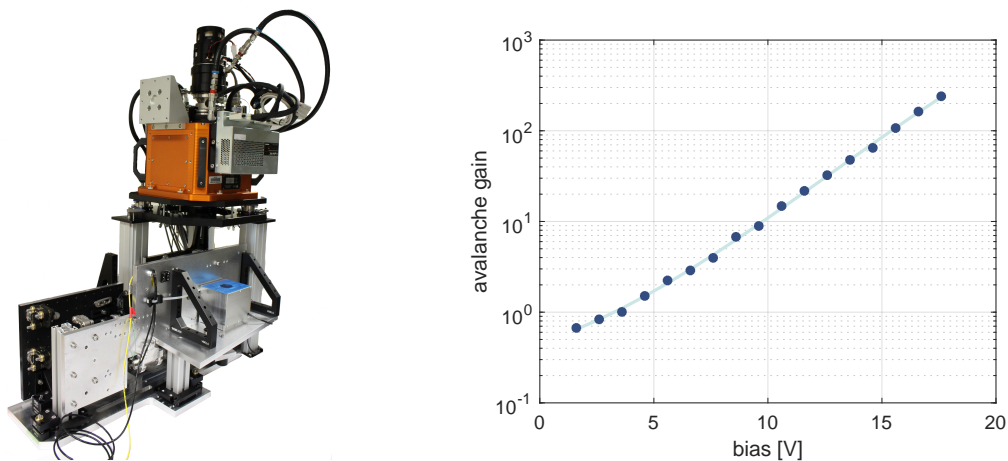


Figure 3. KPIC in the lab. **Left:** KPIC assembled in the adaptive optics lab at IfA Hilo. **Right:** Measurement of the avalanche gain of the SAPHIRA detector used for the Keck pyramid WFS.

3.3 Wavefront control

In September 2018 the KPIC instrument was installed on the Keck II AO bench. After careful alignment with the existing system the instrument was integrated within the Keck AO system, using a dedicated RTC (real-time-controller). This included verifying communication between all the active components and the RTC, and using the internal white light source to calibrate the system and successfully close the loop.

The pyramid RTC uses the wavefront control software CACAO^{12,16} as the basis of the AO control framework. This is based on a series of shared memories which store the real-time AO data (WFS signals, DM commands etc.). Figure 4 shows the engineering GUI currently used with the Keck pyramid WFS and displaying the most relevant data from the sensor and AO system. The key elements are:

1. **Pyramid image.** This is the main image in the top left hand corner and shows the four pupil images that make up the pyramid WFS output.
2. **WFS slopes.** In our case we control the AO system using ‘slope-like’ values computed from the pyramid image using a quad cell formula. This results in two slopes maps, x and y , displayed in the upper right corner.
3. **DM map.** The commands currently applied to the Keck DM. The map is displayed in the ‘DM LOOP Control’ panel. In addition the maximum and minimum of the current commands are displayed.
4. **Residual wavefront map.** This is a map of the residual wavefront as measured by the pyramid WFS, in terms of DM commands. This map is displayed in the ‘WF residual’ panel, which also shows the rms of the residual.
5. **Valid pixel and valid actuator maps.** These are displayed in the ‘Pupil Tracker’ and ‘Reconstructor Mgr’ panels respectively. The valid pixels represent the threshold-ed sum of the 4 pyramid pupils, determining which pixels are illuminated by the Keck pupil. The valid actuators are determined from the valid pixels - actuators which fall outside the illumination of the Keck pupil are not seen during on-sky operation and so are slaved to the average value of their neighbours to protect the DM.

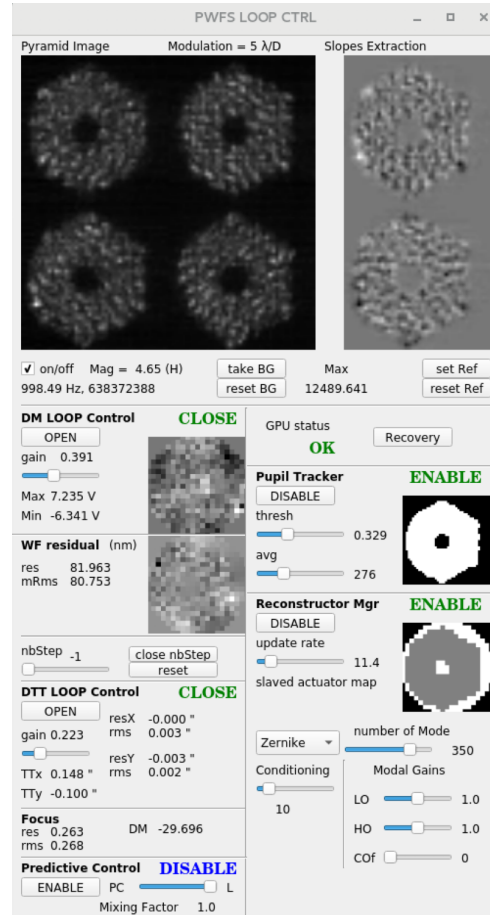


Figure 4. Screenshot of the engineering GUI used for control of the Keck Pyramid WFS during on-sky operation. See text for description.

3.4 Key parameters

The key parameters of the Keck pyramid WFS are summarized in table 1. The wavelength band and wavefront sampling were design choices. The maximum frame rate and effective read noise are determined by the performance of the SAPHIRA detector and the configuration of the readout electronics, with a trade off between high frame rates and low read noise. The throughput was measured during the first on-sky tests.

| Parameter | Maximum frame rate [Hz] | Wavefront sampling (across the pupil) | Wavelength band | Effective read noise [e^-] | Total throughput [%] |
|-----------|-------------------------|---------------------------------------|-----------------|--------------------------------|----------------------|
| Value | 1500 | 40 | H | 0.4 | 9 |

Table 1. Key parameters for the Keck Pyramid wavefront sensor. The noise was measured after installation on the Keck II AO bench, and represents the effective read noise at high avalanche gain (200). The throughput was measured on-sky and represents the total throughput from the source to the electrons read out by the camera, including the quantum efficiency.

4. COMMISSIONING

We successfully closed the loops on-sky with the pyramid WFS during KPICs first light - 20th November 2018 - using two different NGS with magnitudes $H \sim 5.3$ and $H \sim 7.5$. Over the next few months the system performance was gradually improved by careful calibration and optimization of parameters for different conditions and NGS magnitudes. These developments were tested over a series of engineering nights, with the primary performance metric being the image quality on NIRC2 and associated Strehl ratio.

4.1 Performance

Figure 5 shows some examples of K-band images taken with NIRC2 using the pyramid WFS. The hexagonal features of the Keck PSF are clearly visible and these examples represent the image quality achievable with the pyramid WFS for bright H-band stars during good seeing conditions (~ 0.5 arcseconds at 500 nm).

In addition to on-sky engineering nights, science verification nights through July 2019 allowed for shared risk science - testing the performance of the system whilst collecting the first science data with the pyramid WFS. The science results will be the subject of other papers. Here we use these results and those from the engineering nights to assess the performance of the system. Figure 6 shows the K-band Strehl ratio versus guide star magnitude over multiple nights, from first light in November 2018. The results here represent a range of seeing conditions, different developmental stages of the control and calibration procedures, and different elevations/airmass. The different seeing conditions are illustrated by the shaded region showing the expected performance for the range of seeing included over these dates.

Figure 6 illustrates the system working across multiple nights in different conditions. In particular the later nights show the impact of improvements made to the calibration and control of the system, with the later (redder) points generally showing improved performance. The limiting magnitude of the system is determined by a limited throughput of $\sim 9\%$. Sources of throughput loss have been identified and plans to upgrade these components during phase II are in place.

4.2 Preparation for direct imaging science

In addition to integration with the Keck AO system the pyramid WFS required integration with the science instruments. Two types of observations have been performed with the pyramid WFS:

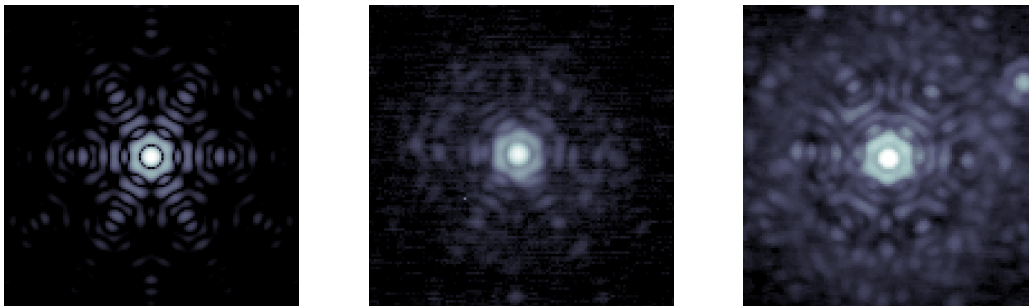


Figure 5. Example on-sky K-band PSFs for the Keck telescope operated with the infrared pyramid WFS. **Left:** perfect theoretical Keck PSF. **Center:** single star observed in December 2018, with $H \sim 6.2$ and a Strehl of 60%. **Right:** binary star observed in June 2019, with $H \sim 5.4$ for the primary and a Strehl of 67%.

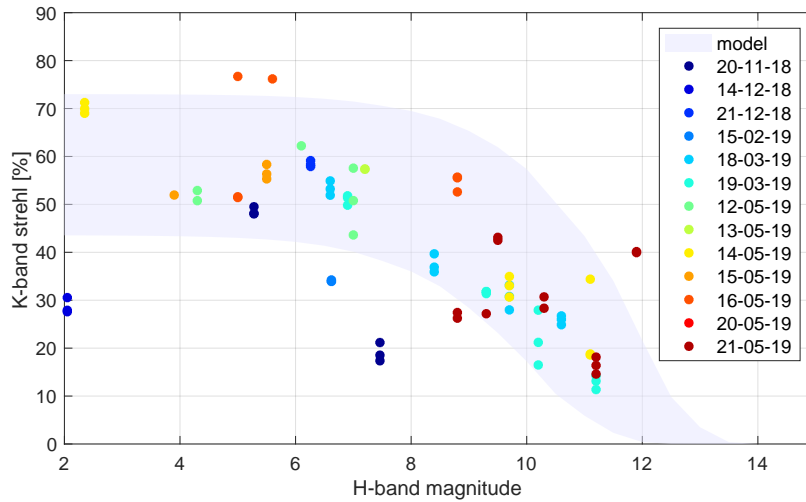


Figure 6. Plot of the K-band Strehl ratio vs. H-band magnitude for different nights of pyramid WFS commissioning (including engineering and science nights). The data encompasses a range of seeing conditions (illustrated by the shaded region) and different stages of the instrument’s development.

1. Imaging with Keck II’s infrared imager (NIRC2), including an L/M-band vortex coronagraph used to suppress the starlight for exoplanet imaging.
2. Spectroscopy of stars and associated planets using the fiber injection unit (FIU) to feed Keck’s infrared spectrograph NIRSPEC.

Here we discuss the integration with NIRC2 and the vortex coronagraph.¹⁷

For effective suppression of starlight using the vortex coronagraph careful control of the beam pointing to reduce tip-tilt errors is required. The Keck pyramid was integrated with NIRC2’s vortex control method QACITS (Quadrant Analysis of Coronagraphic Images for Tip-tilt Sensing).¹⁸ This method uses analysis of the NIRC2 vortex images to adjust the AO pointing offsets in real time and keep the star centred on the vortex. Due to the small linear range of the pyramid WFS - and lack of an independent field steering mirror - these offsets are applied as offsets to the modulator, rather than offsets to the AO loop. Figure 7 shows an example QACITS sequence with the Keck pyramid WFS, using the L-band vortex on-sky.

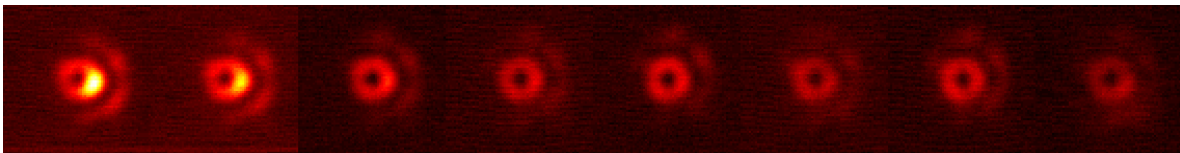


Figure 7. Example of a QACITS sequence with the Keck pyramid WFS, where the target star is centred on the vortex to suppress the star light in the final science image.

5. SCIENCE VERIFICATION

Between April and July 2019, six nights were dedicated to shared risk science with the pyramid WFS. The goal of these nights was to further probe the performance of the sensor for a range of different targets (seeing, elevation and NGS magnitude) while performing the first science observations with the pyramid WFS.

5.1 Comparison with Keck facility adaptive optics

During the course of the science verification process the pyramid WFS was used to observe targets previously observed with the Keck II facility AO system, allowing for performance comparisons with the pyramid WFS.

Figure 8 shows NIRC2 coronagraphic images for the pyramid WFS and Keck II's Shack-Hartmann WFS in NGS mode. In this case the integration time for the pyramid image is one third of that for the Shack-Hartmann image. Nevertheless, the pyramid image clearly displays a better contrast, with less speckles in the low to mid spatial frequencies and a dark hole within the correction band. Figure 9 shows plots of the raw contrast for the two measurements as well as the contrast gain achieved when using the pyramid WFS, for this particular target. Here we observe consistent gains in contrast of between $\sim 2 - 4$ within the correction band (< 0.7 arcseconds). It should be noted that the contrast gain outside the correction band is > 1 , suggesting slightly better seeing

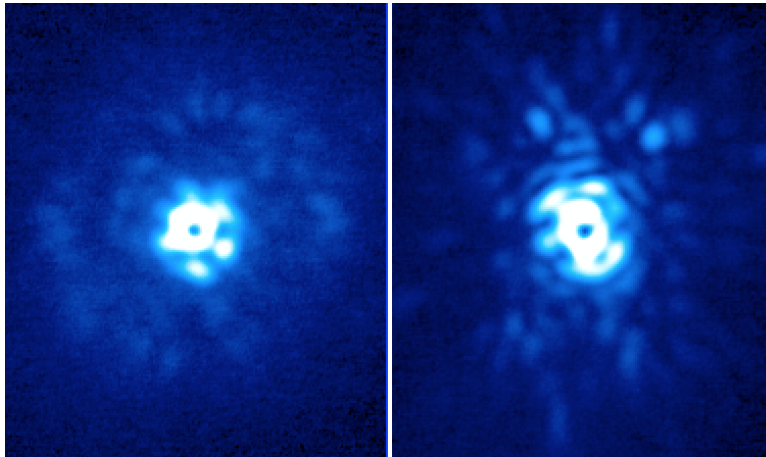


Figure 8. L-band coronagraphic images taken with the pyramid WFS (left) and Shack-Hartmann (right) for the same target on different nights.

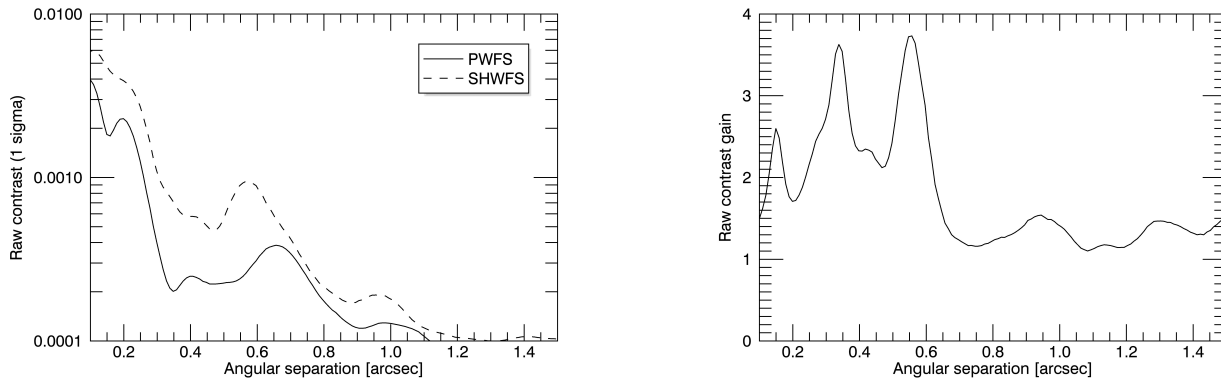


Figure 9. **Left:** Raw post-coronagraphic contrast with Keck II's pyramid WFS and Shack-Hartmann WFS, for the same target on different nights. **Right:** Comparison in contrast between the pyramid WFS and Shack-Hartmann WFS.

conditions on the night the pyramid data was taken. However, this would not account for the magnitude of the gains seen below 0.7 arcseconds. The pyramid has consistently delivered higher contrast over multiple nights of operation.

Many potentially interesting targets for the infrared pyramid WFS would previously only have been observable using Keck II's LGS system. One such target is WISE0720, a brown dwarf binary with $H = 9.9$ and $R = 16.9$. This was previously observed with Keck's LGS system and in April 2019 additional measurements were made with the pyramid WFS. The LGS and pyramid WFS K-band images are shown in figure 10, as well as additional L-band data taken with the pyramid WFS. Comparing the K-band images we find better image quality with the pyramid compared to the LGS system - a FWHM of 5.9 pixels, compared with 6.2 pixels - whilst the conditions for the pyramid observation were slightly worse - 0.7 arcsecond seeing, compared with 0.5 for the previous LGS measurement. These measurements are included in a science paper on this target,¹⁹ and represent the first published science result using the Keck pyramid WFS. It should be noted that the pyramid WFS measurements were taken in April 2019. Since then several improvements to the pyramid WFS control have been made.



Figure 10. NIRC2 images of WISE0720, a brown dwarf binary with 0.35 arcsecond separation. **Left:** K-band image taken with Keck's LGS AO system in October 2018.¹⁹ **Center:** K-band image taken with the pyramid WFS in April 2019. **Right:** L-band image taken with the pyramid WFS in April 2019. In the pyramid images some trefoil is noticeable in the PSFs. This distortion often appears at low elevation and is the subject of on-going investigation.

5.2 Infrared novelty

A unique property of the Keck pyramid WFS is its operation in the near infrared. This allows for high resolution AO correction of some targets which have previously been inaccessible, or very challenging, with Keck's facility AO systems, due to a lack of photons at the visible wavelengths required for either NGS Shack-Hartmann WFS operation and even the LGS tip-tilt control.

Figure 11 summarizes the relative H-band and visible magnitudes of all the stars successfully observed with the Keck pyramid WFS to date. This plot highlights the very faint visible targets which can be reached with this instrument, providing they are sufficiently bright in the infrared.

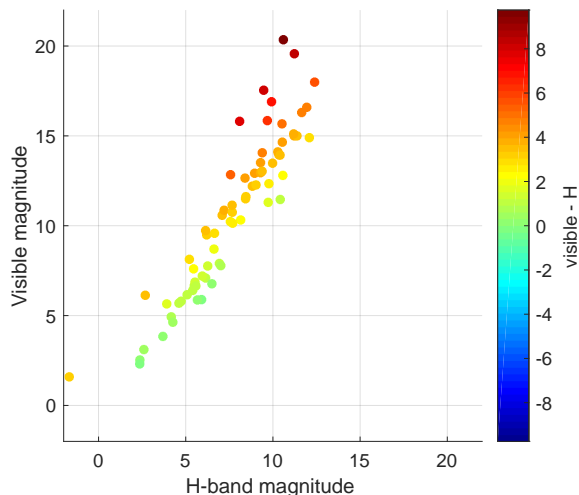


Figure 11. Visible and H-band magnitudes of all the NGS successfully observed with the Keck pyramid WFS, as of June 2019.

6. CONCLUSION

In September 2018 an infrared pyramid WFS was installed on the Keck II AO bench as part of the Keck Planet Imager and Characterizer (KPIC). The sensor is designed to provide high resolution AO correction for faint red objects, to facilitate the search for exoplanets around M-type stars and the study of proto-planetary discs. Here we have reviewed the design and testing of the instrument, and reported on the commissioning and initial science verification.

The pyramid WFS has been operated successfully on-sky over multiple nights since first light in November 2018. Comparison with Keck’s facility AO system has demonstrated an improved performance compared to both NGS and LGS Shack-Hartmann modes. In particular the sensor has demonstrated improved contrast when operated with an L/M-band vortex coronagraph and the infrared imager NIRC2, a promising indication of the direct imaging potential of this system. In addition, the infrared sensor has the ability to operate with very faint visible objects, opening up a range of new science opportunities.

ACKNOWLEDGMENTS

The near-infrared pyramid wavefront sensor is supported by the National Science Foundation under Grant No. AST-1611623. The camera used with the pyramid wavefront sensor is provided by Don Hall with support by the National Science Foundation under Grant No. AST-1106391. The fiber injection unit is supported by the Heising-Simons Foundation.

The W. M. Keck Observatory is operated as a scientific partnership among the California Institute of Technology, the University of California, and the National Aeronautics and Space Administration. The Observatory was made possible by the generous financial support of the W. M. Keck Foundation.

The authors wish to recognize and acknowledge the very significant cultural role and reverence that the summit of Maunakea has always had within the indigenous Hawaiian community. We are most fortunate to have the opportunity to conduct observations from this mountain.

REFERENCES

- [1] Esposito, S., Riccardi, A., Pinna, E., Puglisi, A. T., Quirós-Pacheco, F., Arcidiacono, C., Kompero, M., Briguglio, R., Busoni, L., Fini, L., Argomedo, J., Gherardi, A., Agapito, G., Brusa, G., Miller, D. L., Ramon, J. C. G., Boutsia, K., and Stefanini, P., “Natural guide star adaptive optics systems at LBT: FLAO commissioning and science operations status,” in [*Proceedings of the SPIE*], **8447** (2012).
- [2] Jovanovic, N. et al., “The Subaru coronagraphic extreme adaptive optics system: Enabling high-contrast imaging on solar-system scales,” *Publications of the Astronomical Society of the Pacific* **127**(955) (2015).
- [3] Morzinski, K., Close, L., Males, J., Kopon, D., Hinz, P., Esposito, S., Riccardi, A., Puglisi, A., Pinna, E., Briguglio, R., Kompero, M., Quirós-Pacheco, F., Bailey, V., Follette, K., Rodigas, T., Wu, Y., Arcidiacono, C., Argomedo, J., Busoni, L., Hare, T., Uomoto, A., and Weinberger, A., “MagAO: Status and on-sky performance of the Magellan adaptive optics system,” in [*Proceedings of the SPIE*], **9148** (2014).
- [4] Mawet, D., Wizinowich, P., Dekany, R., Chun, M., Hall, D., Cetre, S., Guyon, O., Wallace, J. K., Bowler, B., Liu, M., Ruane, G., Serabyn, E., Bartos, R., Wang, J., Vasisht, G., Fitzgerald, M., Skemer, A., Ireland, M., Fucik, J., Fortney, J., Crossfield, I., Hu, R., and Benneke, B., “Keck Planet Imager and Characterizer: concept and phased implementation,” in [*Proceedings of the SPIE*], **9909** (2016).
- [5] Mawet, D. et al., “Keck Planet Imager and Characterizer (KPIC): recent results and status update,” in [*Proceedings of the SPIE*], (10703-6) (2018).
- [6] Delorme, J.-R. et al., “A fiber injection unit for Keck: final design and first results,” in [*Proceedings of the SPIE*], (10702-77) (2018).
- [7] Ragazzoni, R., “Pupil plane wavefront sensing with an oscillating prism,” *J. of Modern Optics* **43**, 289–293 (1996).
- [8] Vérinaud, C., “On the nature of the measurements provided by a pyramid wave-front sensor,” *Optics Communications* **233**, 27–38 (2004).

- [9] Wizinowich, P., Chun, M., Mawet, D., Agapito, G., Dekany, R., Esposito, S., Fusco, T., Guyon, O., Hall, D., Plantet, C., and Rigaut, F., “Near-infrared wavefront sensing,” in [*Proceedings of the SPIE*], **9909** (2016).
- [10] Esposito, S., Pinna, E., Puglisi, A., Agapito, G., Véran, J.-P., and Herriot, G., “Non common path aberration correction with non linear WFSs,” in [*Adaptive Optics for Extremely Large Telescopes 4 - Conference Proceedings*], (2015).
- [11] Lilley, S. et al., “A near-infrared pyramid wavefront sensor for Keck adaptive optics: onto-mechanical design,” in [*Proceedings of the SPIE*], (10703-127) (2018).
- [12] Cetre, S. et al., “A near-infrared pyramid wavefront sensor for Keck adaptive optics: real-time controller,” in [*Proceedings of the SPIE*], (10703-119) (2018).
- [13] Plantet, C. et al., “Keck II adaptive optics upgrade: simulations of the near-infrared pyramid sensor,” in [*Proceedings of the SPIE*], (10703-115) (2018).
- [14] Goebel, S. B., Hall, D. N. B., Guyon, O., Warmbier, E., and Jacobson, S. M., “Overview of the SAPHIRA detector for adaptive optics applications,” *Journal of Astronomical Telescopes, Instruments, and Systems* **4**, 4 – 4 – 10 (2018).
- [15] Atkinson, D. E., Hall, D. N. B., Baker, I. M., Goebel, S. B., Jacobson, S. M., Lockhart, C., and Warmbier, E. A., “Next-generation performance of SAPHIRA HgCdTe APDs,” in [*Proceedings of the SPIE*], **9915** (2016).
- [16] Guyon, O. et al., “The compute and control for adaptive optics (CACAO) real time control software,” in [*Proceedings of the SPIE*], (10703-51) (2018).
- [17] Xuan, W. J., Mawet, D., Ngo, H., Ruane, G., Bailey, V. P., Choquet, É., Absil, O., Alvarez, C., Bryan, M., Cook, T., Castellá, B. F., Gonzalez, C. G., Huby, E., Knutson, H. A., Matthews, K., Ragland, S., Serabyn, E., and Zawol, Z., “Characterizing the performance of the NIRC2 vortex coronagraph at W. M. Keck Observatory,” *The Astronomical Journal* **156**(4) (2018).
- [18] Huby, E., Absil, O., Baudoz, D. M. P., Castellá, B. F., Bottom, M., Ngo, H., and Serabyn, E., “The QACITS pointing sensor: from theory to on-sky operation on Keck/NIRC2,” in [*Proceedings of the SPIE*], **9909** (2016).
- [19] Dupuy, T. et al., “WISE J07200846B Is A Massive T Dwarf,” *The Astronomical Journal - accepted for publication* (2019).